PHYSICAL REVIEW C VOLUME 24, NUMBER 5 NOVEMBER 1981

Nuclear spallation-fragmentation reactions induced by high-energy projectiles

X. Campi* and J. Hüfner
Institut für Theoretische Physik der Universität Heidelberg
and Max-Planck-Institut für Kernphysik, Heidelberg, Federal Republic of Germany
(Received 13 April 1981)

In a fragmentation or spallation reaction a target nucleus is hit by a high-energy projectile (proton or heavy ion). In the fast step of the reaction highly excited intermediate nuclei, the prefragments, are formed. They decay to the particle stable final fragments in a second step. We treat the first step in Glauber theory. For the decay chain we propose a master equation and solve it by converting it to a differential equation. Analytical solutions are obtained. They clarify the underlying physics: The mass yield curve $\sigma(A)$ of the final fragments is directly related to the distribution of excitation energy in the prefragments. The isobaric cross sections $\sigma(A,N\text{-}Z)$ for fixed A are dominated by the level density of the final fragment at its lowest particle threshold. Some properties of the target, like its neutron excess, enter via a memory factor. The formulas are successfully compared to the data.

[NUCLEAR REACTIONS Spallation and fragmentation reactions; projectile protons of several GeV, various targets; theory for cross sections; two step model; fast step Glauber theory; analytical formula for evaporation chains.]

I. INTRODUCTION

A proton or heavy ion with high energy strikes a target nucleus. This nucleus then disintegrates into smaller fragments. What is the physics? Many experiments have been or are still being performed to study this problem and a wealth of data has been accumulated. Protons as projectiles are used with energies between several hundred MeV and 400 GeV and heavy ions up to the presently available energy of 2 GeV/nucleon. Target nuclei range from relatively light elements, like Fe, to uranium. The cross sections $\sigma(A,N\text{-}Z)$ for the residual nuclei are usually measured by radio-chemical methods or with a mass spectrometer. We refer only to a few recent papers,[1-5] from which the earlier literature can be traced, and to a collection[6] of articles on spallation reactions. At present, research focuses on the momentum distributions of the fragments[1] and also coincidence measurements between two fragments are performed.[7] The data on the spallation and fragmention cross sections (we use the terms "spallation" and "fragmentation" as synonyms) exhibit the following regularities:

(i) There are some but no dramatic differences between the results with protons and heavy ions as projectiles.[5]

(ii) One observes all particle stable fragment nuclei with mass smaller than the target. For particle energies in the GeV region, the mass yield curve $\sigma(A)$ varies smoothly with A and is usually of the order of $10-20$ mb[1,5].

(iii) For a given element Z the cross sections $\sigma(Z,N)$ for the fragment isotopes show the shape of a bell, if $\ln\sigma(Z,N)$ is plotted against N. The maximum occurs for the most bound isotope[5,8,9]

(iv) The fragment cross sections $\sigma(Z,N)$ for a given isotope goes rapidly up with increasing projectile energy until about a few GeV from whereon it saturates.[4]

The experimental cross sections can be successfully parametrized by empirical formulas.[10,11]

There are also some phenomenological approaches to the data.[12,13] But really, what is the essential physics of these reactions? The two-step model, proposed by Serber,[14] is still the accepted framework: In a first fast step of the reaction the projectile knocks a few nucleons out of the target nucleus and generates a distribution of prefragments, which are highly excited. The prefragments then decay in a second step by emitting nucleons or light nuclei or by fissioning, until the final particle stable fragment nuclei are reached. The two-step model is usually realized by an intranuclear cascade calculation[15] for the fast part of the reaction, and a chain of compounds nucleus decays[16] for the second step. Fission is usually left out of the description. The salient features of the data are mostly reproduced. But, in our opinion, the extremely complicated numerical calculations do not permit sufficient insight into the physics. For instance, which are relevant and which are redundant assumptions and parameters?

Therefore, we prefer a different approach. While we accept the general framework of the two-step model, we realize it differently. We insist on analytical results. Thus, our solutions are complementary to the computer-oriented intranuclear cascade and compound-chain calculations. Since the underlying model is the same, the numerical results should be and are similar. Why do we dare to look for a simple description of a complicated process such as fragmentation reactions? A simple description works *because* the process is extremely complicated. Look at themodynamics, for example, or Bohr's theory of the compound nucleus reaction. Of course, one can expect only simple answers for simple questions. Thermodynamics, for instance, describes well the behavior of a few macroscopic variables, like the average energy, but to calculate exactly the path of the electron in a solid would be impossible. We think that a similar situation is realized for fragmentation reactions. Therefore, instead of following the microscopic details of the reaction we consider only a few "macroscopic" variables, like nucleon number or excitation energy, whose time evolution we describe. The direction in which the system proceeds is largely determined by phase space (or level density) and to a smaller degree by the dynamics (matrix elements). If time suffices to reach thermal equilibrium, the results should be completely independent of the dynamics.

We use Glauber theory to determine the prefragment distribution in the space of the macroscopic variables. Then for the second step we propose a master equation in the few variables under consideration. We have not included fission. Therefore, in the comparison with experiment we mostly restrict ourselves to target nuclei with $A_T \lesssim 100$. Yet, our formulas for the isotope distributions often also work for fragments which are presumably created in fission events. The reason may lie in the thermal nature of the reaction: The isotope distributions are determined by the level density of the final nuclei and on very little else. In this paper we restrict ourselves to a theory of the fragment *cross sections* $\sigma(Z,N)$ for reactions in which the incident projectile has an energy in the GeV region. We present a theory of the fast step in the next section, then we describe the decay chain in Sec. III. In Sec. IV. we compare with experiment and we close with a conclusion.

II. THE FAST STEP

A high energy proton ($E > 1$ GeV) traverses a nucleus essentially on a straight line. On its way it collides with several target nucleons, transfers energy and momentum to them, and may excite them into higher baryonic states. Depending on the place where they have been struck, the recoiling nucleons either escape directly or collide with a few other nucleons and transfer energy to them. Some of these may leave the nucleus. We do not follow the evolution of the system, but rather postulate: The distribution of excitation energy in the prefragment depends only on the number of primary interactions between the projectile proton and the target nucleons. The cross section σ_n for n primary collisions can be calculated[17] as

$$\sigma_n = \int d^2b \frac{T^n(\vec{b})}{n!} e^{-T(\vec{b})} , \tag{2.1}$$

where the function

$$T(\vec{b}) = \int \frac{dz}{\lambda} \frac{\rho(\vec{b},z)}{\rho(0)} \tag{2.2}$$

measures the thickness of the target at the impact parameter $(\vec{b})$ in units of the mean free path λ. ($\lambda = 1.5$ fm above 1 GeV.) The total reaction cross section σ_R is simply the sum of the σ_n ($n \geq 1$). We assume an exponential e^{-E/E_0} for the distribution of energy deposited into the prefragment by one projectile collision. E_0 is the mean energy transferred. Then the distribution $F_n(E)$ after n collisions arises by properly folding the exponentials

$$F_n(E) = \frac{1}{(n-1)!}\frac{E^{n-1}}{E_0^n}e^{-E/E_0} . \quad (2.3)$$

The cross section for the projectile to deposit an energy E into the prefragment is then

$$\frac{d\sigma_P}{dE} = \sum_{n\geq 1}\sigma_n F_n(E) . \quad (2.4)$$

For a uniform target density with radius R_T the integral Eq. (2.1) can be performed to

$$\sigma_n = \frac{\pi}{2}\lambda^2(n+1) \quad (2.5)$$

for $1 \leq n \leq 2R_T/\lambda$ and zero elsewhere. The number of nucleons which is removed from the target in the first step also depends on the number n of primary projectile collisions. We denote by $\langle n \rangle$ the mean number of primary interactions

$$\langle n \rangle = \frac{\sum n\sigma_n}{\sigma_R} . \quad (2.6)$$

If the nucleon number A of the final fragments (i.e., after the second step) is sufficiently far from the target mass number A_T (i.e., if $A_T - A << \langle n \rangle$), then the distribution of prefragments in A and $I = N\text{-}Z$ need not be known exactly. We can approximate it by functions peaked around the *mean* values A_0 and I_0 of the prefragment distributions, for instance,

$$\frac{d\sigma_P}{dE}(A,I,E) = \delta_{A,A_0}\delta_{I,I_0}\sum_{n\geq 1}\sigma_n F_n(E) , \quad (2.7)$$

where we assume $A_T - A_0 = \gamma\langle n \rangle$ and $I_T - I_0 = \gamma'\langle n \rangle$. The constants of proportionality γ and γ' are of order 1 or 2.[15] If heavy ions are used as projectiles, the σ_n should be calculated from an abrasion-ablation calculation.[18]

III. THE DECAY CHAIN

After the fast step, all prefragments are not in one defined quantum state. Depending on details of the formation history each prefragment nucleus is in a different quantum state, whose precise properties we do not know. Therefore, the prefragments can be viewed as an ensemble. We classify and group the members of this ensemble according to a few macroscopic variables like mass number A, neutron excess I, excitation energy E, and maybe a few others. The probability to find the system in a class characterized by (A, I, E, etc.), is then

$$P(A,I,E,\ldots;t=0) = \frac{1}{\sigma_R}\frac{d\sigma_P}{dE}(A,I,E,\ldots) , \quad (3.1)$$

where σ_R is the reaction cross section and $d\sigma_P/dE$ denotes the cross section to form a prefregment in this class. We indicate by "$t = 0$" the time at the end of the fast step. Then ($t > 0$) the system evolves to rid itself of the excitation energy. We describe this evolution by a master equation

$$\dot{P}(\vec{x};t) = -P(\vec{x};t)\int d\vec{y}M(\vec{x}\rightarrow\vec{y})\Omega(\vec{y}) + \int d\vec{y}\,P(\vec{y};t)M(\vec{y}\rightarrow\vec{x})\Omega(\vec{x}) , \quad (3.2)$$

where $\vec{x} = (A, I, E\ldots)$. The functions $M(\vec{x}\rightarrow\vec{y})$ describe the dynamics (mean squared matrix elements) for going from class $\vec{x}$ to class $\vec{y}$. The number of states in each class is denoted by the density of states $\Omega(\vec{x})$. In order that a master equation in the macroscopic variables $\vec{x}$ applies, the dynamics must not depend on properties of the individual quantum states of the system, but only on some average quantities like $\vec{x}$. The use of a master equation and the limitation to the macroscopic variables (A,I,E) is our basic assumption in this paper.

After a long time (long on the scale of strong interactions) all particle decays have ceased and particle stable fragments have been formed. Their cross section is related to the solution of Eq. (3.2) by

$$\sigma(A,I) = \sigma_R\int_0^{E_t(A,I)} dE\;P(A,I,E;t\rightarrow\infty) , \quad (3.3)$$

where the integral over E extends to $E_t(A,I)$, the lowest particle threshold, and samples the probability from all particle stable states of the isotope characterized by A and I.

In order to solve Eq. (3.2), we integrate it over t from $t = 0$ to $t = \infty$ and introduce the notation

$$W(\vec{x}) = \int_o^\infty dt\;P(\vec{x};t) . \quad (3.4)$$

The resulting equation in the P's can be split into two parts: If the excitation energy $E < E_t(A,I)$ the system is stable and the matrix elements $M(E\rightarrow E') = 0$. Then we have

$$P(\vec{x};t\rightarrow\infty) = P(\vec{x};0) + \Omega(\vec{x}) \times\int d\vec{y}\;W(\vec{y})M(\vec{y}\rightarrow\vec{x}) . \quad (3.5)$$

In the other case, $E > E_t(A, I)$, the system is unstable and $P(\vec{x};t\rightarrow\infty) = 0$. We get

$$W(\vec{x})\int d\vec{y}\; M(\vec{x}\to\vec{y})\Omega(\vec{y}) - \int d\vec{y}\; W(\vec{y})M(\vec{y}\to\vec{x})\Omega(\vec{x}) = P(\vec{x};0)\ . \tag{3.6}$$

Equation (3.6) is an inhomogeneous integral equation for $W(\vec{x})$, the driving term being the prefragment distribution $P(\vec{x};0)$. The solution of Eq. (3.6) is inserted into Eq. (3.5) and this result is used to compute the distribution of fragments Eq. (3.3). We defer the detailed solution of Eq. (3.6) to the Appendix, but introduce here the notation which is necessary to understand the results. The level density $\Omega(\vec{x})$ is related to the entropy $S(\vec{x})$ by

$$S(\vec{x}) = \ln\Omega(\vec{x})\ . \tag{3.7}$$

The derivatives of S are denoted in the thermodynamic way

$$\begin{aligned}\frac{\partial S}{\partial E} &= \frac{1}{T} \equiv \beta\ ,\\ \frac{\partial S}{\partial N} &= -\beta\mu_N\ ,\\ \frac{\partial S}{\partial Z} &= -\beta\mu_Z\ ,\end{aligned} \tag{3.8}$$

with the temperature T and the chemical potentials μ. For the dynamics contained in the function $M(\vec{x}\to\vec{y})$ we consider neutron, proton, and α decay. It turns out (cf. Appendix) that we do not need to know the precise form of M but that the solution depends only on certain mean values of M. For example, we denote by

$$\langle\delta\vec{x}\rangle = \int d\vec{y}(\vec{x}-\vec{y})M(\vec{x}\to\vec{y}) \Big/ \int d\vec{y}\; M(\vec{x}\to\vec{y}) \tag{3.9}$$

the average value for the change in $\vec{x}$ in one decay of the system. When calculating numerical values for the relevant mean values, we use the compound nucleus model. But the final formulas do not depend very sensitively on these mean values and not too large deviations from compound nucleus decays can hardly be detected. Similarly, inclusion of other decay models, like d or t emission, will only modify the averages. In compound decay theory,[19] neutron, proton, and α decay enter with their statistical weights $(2s+1)$, i.e., with $\frac{2}{5}$, $\frac{2}{5}$, and $\frac{1}{5}$, respectively. Then the mean chage α of the nucleon number in one decay is

$$\alpha = \langle\Delta A\rangle = \tfrac{2}{5}\cdot 1 + \tfrac{2}{5}\cdot 1 + \tfrac{1}{5}\cdot 4 = \tfrac{8}{5}\ . \tag{3.10}$$

The mean change in neutron excess

$$\tau_1 = \langle\Delta I\rangle = \tfrac{2}{5}(-1) + \tfrac{2}{5}(+1) + \tfrac{1}{5}0 = 0\ . \tag{3.11}$$

The mean loss in excitation energy

$$\epsilon = \langle\Delta E\rangle = \tfrac{2}{5}(S_n + T) + \tfrac{2}{5}(S_P + T + V_C) + \tfrac{1}{5}(S_\alpha + T + 2V_C) \simeq 20\ \text{MeV} \tag{3.12}$$

is calculated form the separation energies S_i, the mean kinetic energy (equalling the temperature T), and the Coulomb barrier[19] V_C. The value 20 MeV corresponds to nuclei around $A = 60$ and a temperature $T = 4$ MeV. The mean-square change in $(N\text{-}Z)$ is given by

$$\tau_2 = \langle(\Delta I)^2\rangle = \tfrac{2}{5} + \tfrac{2}{5} + 0 = \tfrac{4}{5}\ . \tag{3.13}$$

With this notation the main results of our paper can be stated in the following form.

The *mass dispersion yield* $\sigma(A)$ [(i.e., $\sigma(A,I)$ summed over all isobars]

$$\sigma(A) = \frac{E_t(A)}{\alpha}\frac{d\sigma_P}{dE}[A_0, I_0, \frac{\epsilon}{\alpha}(A_0 - A)] \tag{3.14}$$

is directly related to the *distribution of excitation energy* of the initial *prefragments*. A_0 and I_0 are the mean values for the prefragment nucleon number and neutron excess, respectively. The lowest particle threshold $E_t(A)$ (that of the most bound isobar) arises from the integration over E in Eq. (3.3). The physics of Eq. (3.14) is very simple: Consider a prefragment with A_0 and excitation energy E being formed in the first step of the reaction with cross section $d\sigma_P/dE$. It decays. In each step its energy is reduced by ϵ and its particle number by α (on the average). Therefore, it has reached a particle stable nucleus with mass number A, if

$$\epsilon(A_0 - A)/\alpha \simeq E\ , \tag{3.15}$$

which is the argument in Eq. (3.14). The cross section for fragment A equals the formation cross section of the prefragment with excitation energy E, since no probability is lost during the cascade. We have assumed ϵ to remain constant. In an actual decay chain the average value ϵ may decrease somewhat during the cascade.

The *isobaric cross section* $\sigma(A,I)$ for fixed A is given by

$$\sigma(A,I) = c(A)\frac{\Omega[A,I,E_t(A,I)]}{\Omega[A,I_s,E_t(A,I_s)]} \times \left[\exp - \frac{(I-I_0)^2}{2\tau_2(A_0-A)/\alpha}\right]\sigma(A) . \tag{3.16}$$

It contains the factor $\sigma(A)$ from Eq. (3.14) and a normalization constant $c(A)$ chosen to ensure $\sum_I \sigma(A,I) = \sigma(A)$. The main physics resides in the *level density* factor and in the Gaussian which we call the *"memory factor."* we discuss them in detail: In the numerator of Eq. (3.16) is the level density $\Omega[A,I,E_t(A,I)]$ of the fragment under consideration (with nucleon number A and neutron excess $I = N\text{-}Z$) taken at the energy of the *lowest* particle threshold $E_t(A,I)$ of this particular isotope. We have divided by the corresponding level density of the most bound isobar with $I = I_s$. Except near closed shells, the level densities $\Omega(A,I,E)$ depend only weakly on I but increase rapidly with excitation energy E. For instance, in the Fermi gas model

$$\Omega(A,I,E) \sim e^{2\sqrt{a}\sqrt{E}} , \tag{3.17}$$

where the level density parameter $a \approx A/8$ MeV^{-1}. The exponential dependence on the excitation energy in Eq. (3.17) is the crucial factor in the isobaric distribution of Eq. (3.16). For example, it is responsible for the bell shaped isotopic cross sections. The level density factor is the "thermal part" of the reaction, it depends only on the properties of the observed fragment but not at all on the "history" (which target and which decay mechanism). The memory factor, Gaussian in the distance $(I\text{-}I_0)$ to the mean neutron excess of the prefragment, remembers some properties of the prefragment. However, because of the factor $(A_0 - A)$ the memory is washed out the further away the final fragment is from the prefragment. Finally, as already discussed above, the factor $\sigma(A)$ is directly related to the prefragment distribution. Thus Eqs. (3.14) and (3.16), the main equations of our paper, show the salient features. The mass yield curve $\sigma(A)$ is directly related to the prefragment distribution because of conservation of probability and energy, essentially. *Thermalization,* i.e., loss of memory, characterizes the isobaric (and also the isotopic) distributions of the cross sections. Note the absence of adjustable parameters in Eqs. (3.14) and (3.16).

IV. COMPARISON WITH EXPERIMENT

The prediction Eq. (3.14) for the mass yield curve $\sigma(A)$ and the relation Eq. (3.16) for the isobaric (and isotopic) distributions of fragments are the central results of our paper. They are clear and transparent in their physics, but how well do they work? We begin with the mass yield curve $\sigma(A)$. It is related [Eq. (3.14)] to the distribution of excitation energies in the prefragment $d\sigma_P/dE$, whose form is given in Eq. (2.7). There the only free parameter is E_0, the mean energy transferred to the prefragment when the projectile collides with one target nucleon. The parameter E_0 may depend on the incident energy. A value of the order of 100 MeV seems reasonable.[15,18] All other quantities, the σ_n [Eq. (2.1)] and the mean values α and ϵ [Eqs. (3.10) and (3.12)] are given. For a comparison with experiment we have chosen the mass yield curve $\sigma(A)$ for the reaction 300 GeV protons on Ag. Figure 1 shows a comparison between experiment[5] and our prediction. With $E_0 = 100$ MeV the trend of the data as well as the absolute magnitude are reproduced. The agreement is as good as obtained in an intranuclear cascade calculation followed by an evaporation chain.[5]

We turn to the isobaric and isotopic distributions for the fragments [Eq. (3.16)]. We try to investigate separately the level density factors and the memory part. First, fragments are considered which are very

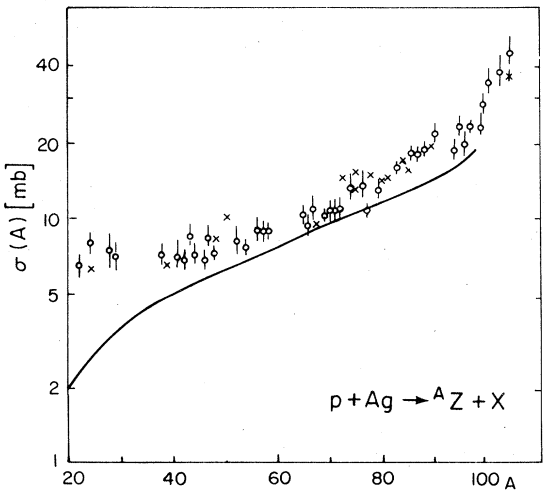

FIG. 1. The mass yield curve $\sigma(A)$ against the nucleon number A of the produced fragments. The points are from an experiment (Ref. 5) where Ag is bombarded with 300 GeV protons. The solid line represents the prediction.

far removed from the target (Na and K isotopes produced by 20 GeV protons on uranium). Therefore, they should have little memory and their distribution should reflect the density of state factors most clearly. Figure 2 shows two examples. There the ratio

$$\frac{\sigma(Z,N)}{\sigma(Z,N_s)} = \frac{\Omega[Z,N,E_t(Z,N)]}{\Omega[Z,N_s,E_t(Z,N_s)]} \tag{4.1}$$

is plotted. Only isotopic cross sections are compared, normalized to the cross section $\sigma(Z,N_s)$ of the most bound isotope. The level densities in Eq. (4.1) are directly obtained by counting levels with their spin degeneracies $(2J+1)$ as given in the level scheme.[20] Sometimes an extrapolation using the exponential form Eq. (3.17) has been necessary. According to Fig. 2 the prediction follows the experimental curves except on the low A side. Here the thresholds and, therefore, the level densities are so small that statistical arguments may no longer be valid. For instance, in ^{21}Na the threshold is at 2.4 MeV, and there are just 20 particle stable states [counted with their degeneracy $(2J+1)$].

For most nuclei, especially the heavier ones, level densities are not directly available, and if measured, they are usually known only for two isotopes. Therefore, calculated or parametrized level densities have to be used. For instance, in the Fermi gas model the level density at the threshold energy E_t is proportional to

$$\Omega(A,I,E_t) = \Omega(A,I,0)e^{2(aE_t)^{1/2}}, \tag{4.2}$$

where the level density factor a increases with nucleon number A roughly like $a = A/8$ MeV^{-1}.

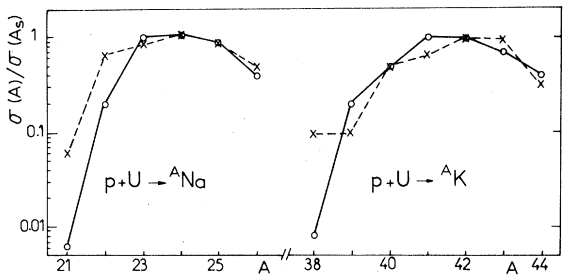

FIG. 2. The influence of the level density on the final fragment cross section, a test of relation (4.1). The isotopes Na and K are produced by bombarding U with 20 GeV protons (Refs. 22 and 23). The experimental cross sections (open circles) are normalized to the one of the most bound isotope. The crosses are our predictions using experimentally determined level densities.

Figure 3 shows a comparison between the experimental isotope distribution for Na and the prediction Eq. (4.2), where the experimental[24] energies for the lowest particle threshold are used. The coefficient $\Omega(A,I,0)$ has been taken constant and $a = 2.25$ MeV^{-1}. For most isotopes the calculated cross sections follow the experimental ones, but calculated even-odd effects are more pronounced than in the data. Furthermore, for the very neutron rich isotopes (heavier than ^{30}Na) the simple formula Eq. (4.2) fails completely. We do not know the reason, maybe statistical arguments break down.

The ratio of level densities in Eq. (4.1) can also be parametrized in a more model-independent fashion,[21] using the thermodynamic relations (3.7) and (3.8)

$$\frac{\sigma(Z,N)}{\sigma(Z,N_s)} = \frac{\Omega[Z,N,E_t(Z,N)]}{\Omega[Z,N_s,E_t(Z,N_s)]}$$

$$= \exp\{\beta[E_t(Z,N) - E_t(Z,N_s)] - \mu_N(N-N_s)\}, \tag{4.3}$$

where β and μ_N are adjustable parameters. Of

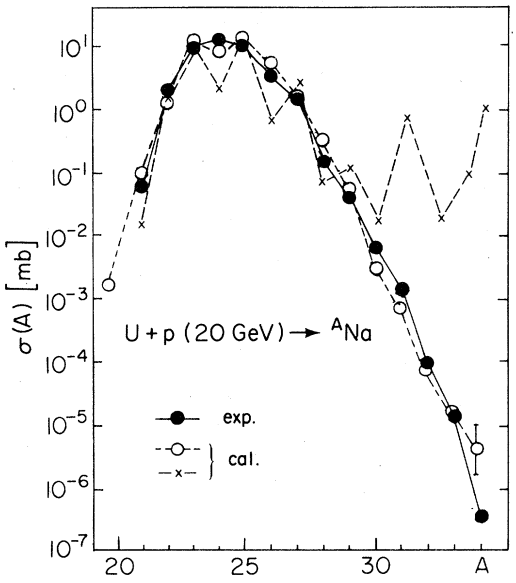

FIG. 3. The experimental cross sections (Ref. 22) (solid points) for the Na isotopes (p + U at 20 GeV) are compared with the calculation. Two models for the level densities have been assumed. The crosses correspond to the Fermi gas model, Eq. (4.2), the open circles arise from a two parameter fit of a thermodynamic expression for the level density, Eq. (4.3).

course, in this relation the two threshold energies $E_t(Z,N)$ and $E_t(Z,N_s)$ have to be taken with respect to the same reference energy, e.g., including the total binding energy[24] of each nucleus. We use Eq. (4.3) to make a least square fit to $\ln\sigma(Z,N)$ of the Na isotopes. The parameters take values $\beta = 0.5$ MeV^{-1} and $\mu_N = 7.8$ MeV. The fit to the data is excellent (Fig. 3) and covers essentially the whole range. The error bar in the calculated value of ^{34}Na represents uncertainties in the experimental binding and neutron separation energies.

What is the physical significance of the temperature $T = \beta^{-1}$ and of the chemical potential μ_N? For μ_N the answer is easy: Its value of 7.8 MeV obtained in the fit corresponds well to the lowest threshold in the valley of stability. According to the Fermi gas model the excitation energy E^*, which corresponds to the temperature T, is given by

$$E^* = aT^2 , \tag{4.4}$$

with the level density factor a. For $\beta = 0.5$ MeV^{-1}, $T = 2$ MeV one finds $E^* = 12$ MeV. Thus, the excitation energy is very small. It essentially corresponds to the threshold energy of the *final* fragment. Therefore, the temperature β has *nothing* to do with the excitation energy of the *initial* state of the reaction.

Since the physics is clear, we can turn the argument around. We identify $E^* = \mu_N$ and then have an experimental determination of the level density factor

$$a_{\text{exp}} = \mu_N\beta^2 , \tag{4.5}$$

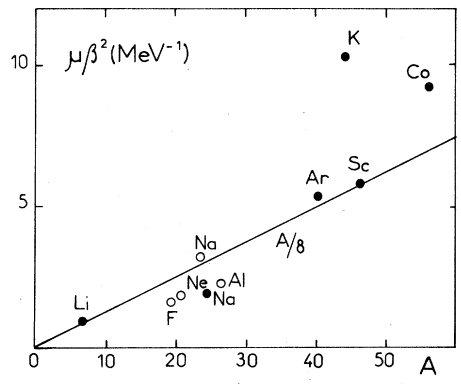

FIG. 4. The parameter $\mu\beta^2$, which equals the level density parameter a_{exp}, Eq. (4.5), as a function of the mass number A of the most bound isoptope. The points arise from fitting cross sections with the expression Eq. (4.3) for the level density. Heavy dots: p + U reactions, open circles ^{40}Ar + ^{12}C (Ref. 25). The "standard law" $a = A/8$ is also represented.

where the values of μ_N and β are obtained from a fit to fragment cross sections. Figure 4 shows the "experimental" level density factors a_{exp} as a function of the mass number A for a number of reactions. On the whole, the empirical law $A/8$ is recovered. This is, we think, another independent support for our claim that the isobaric and isotopic cross sections are dominated by the level density at the lowest particle threshold in the final fragment.

The isobar distribution $\sigma(A,I)$ "remembers" the mean neutron excess of the prefragment via the Gaussian in Eq. (3.16). The width of the Gaussian is given by $2(A_0 - A)\tau_2/\alpha$, where the parameters τ_2 and α are calculated in Eqs. (3.10) and (3.13), $2\tau_2/\alpha = 1$. In order to test the memory effect, the level density dependence has to be eliminated, e.g., by comparing cross sections of isobaric fragments produced from several isobaric targets. Then the dependence on I_0, the neutron excess of the prefragment, is given by

$$\ln\frac{\sigma(A,I)}{\sigma(A,I')} = c + \frac{(I - I')\cdot\alpha}{(A_0 - A)\tau_2}\cdot I_0 , \tag{4.6}$$

where the constant c is independent of I_0. The ratio of cross sections depends linearly on I_0, the slope being a function of the neutron excesses I and I' of the fragment isobars. In Fig. 5 the prediction (4.6) is compared with experiment[8]: 1.8 GeV protons strike ^{96}Zr, ^{96}Mo, and ^{96}Ru as targets and the isobars at $A = 72$ are observed. Indeed, the data exhibit a linear dependence on I_0 (which we identified with the neutron excess of the target). The slopes of the straight lines are calculated from Eq. (4.6) ($A_0 - A = 20$). They fit the data well and even reproduce the change from increasing to decreasing slope, if $I - I'$ becomes negative. To our knowledge, Eq. (4.6) is the first quantitative prediction of the memory effect.

Figures 6–8 show the combined effect of level density and memory factors. Figure 6 shows again very clearly the influence of the target composition. Three isotopes of Mo have been bombarded by 720 MeV alpha particles and the fragment nuclei in the region of $A = 70$ are observed. If the fragment cross sections are plotted against the ratio N/Z of the final fragment, three distinctly displaced bells arise. The curves are parabolic fits to the calculated cross sections. They contain the memory factor and the thermodynamic expression for the level densities. The parameters β, μ_N and μ_Z for the best fit vary by about 10% going from ^{92}Mo to ^{100}Mo, average values being $\beta = 1.0$ MeV^{-1}, $\mu_N = 9.1$ MeV, and $\mu_Z = 7.0$ MeV.

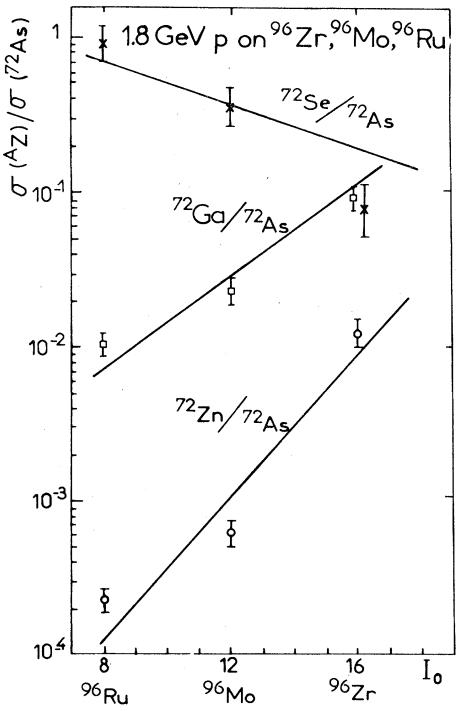

FIG. 5. Test of the "memory effect." The ratio of cross sections for fragment isobars is plotted against $I_0 = (N - Z)$ of the target nucleus. Experiment from Ref. 8. The slope of the straight lines is the parmeter-free prediction of Eq. (4.6), the additive constant of the straight lines has been adjusted by eye.

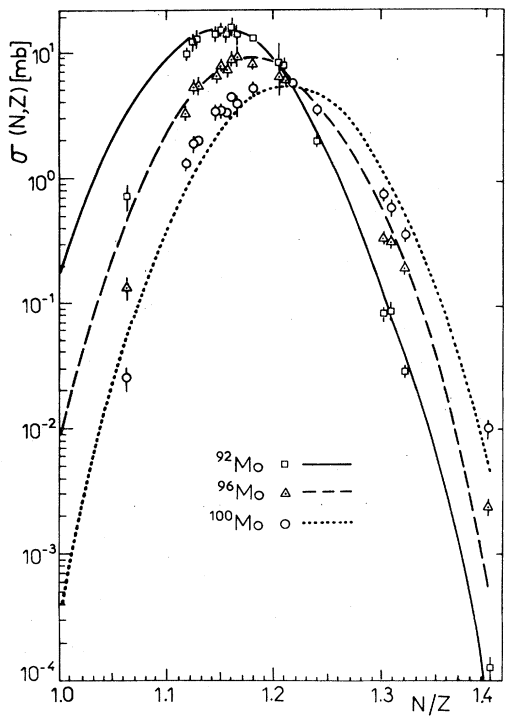

FIG. 6. Spallation of molybdenum isotopes ^{92}Mo, ^{96}Mo, and ^{100}Mo by 0.7 GeV alpha particles producing nuclei around $A = 70$. The cross sections (Ref. 9) are plotted against the ratio N/Z of the fragment. The curves are parabolic fits to the calculated cross sections including level density and memory factors. The heights of the three curves are adjusted.

Figure 7 shows an example of a heavy ion reaction[25]: ^{12}C is bombarded by 213 MeV/nucleon. ^{40}Ar and the projectile fragments are detected. The experimental isotope cross sections for three elements are compared to the calculation. The values $\beta^2\mu_N$ obtained from the fit to the data are entered into Fig. 4 and follow the trend. The agreement with the data is fair, again the calculation shows too much structure.

So far, we have deliberately restricted the discussion to fragment nuclei below $A = 100$. For heavier nuclei we observe irregularities which we have not been able to resolve. Figure 8 shows an example. The trends of the data but not the structure are reproduced. The values of the chemical potentials are $\mu_N = 9.5$ MeV and $\mu_Z = 4.0$ MeV and the "temperature" $\beta^{-1} = 1.3$ MeV. The small value of μ_Z with respect to μ_N indicates that some effects related to the Coulomb potential have been neglected in our calculation. The temperature $T = \beta^{-1}$ is too large by a factor of 2, if compared to the relation (4.5). We do not know the reason.

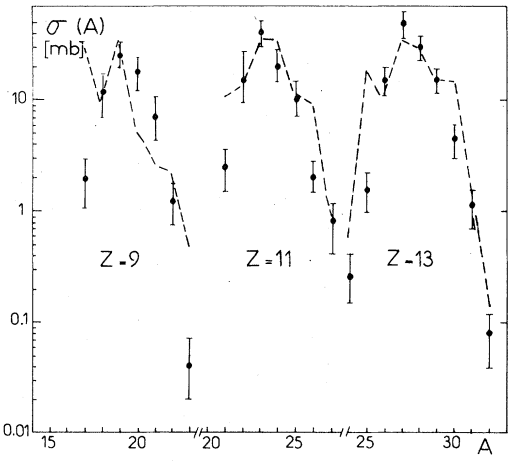

FIG. 7. Projectile fragmentation in the reaction ^{40}Ar + ^{12}C at 213 MeV/nucleon. The data (solid points) are from Ref. 25, the calculation is represented by the dashed line. The absolute magnitude is adjusted for each element.

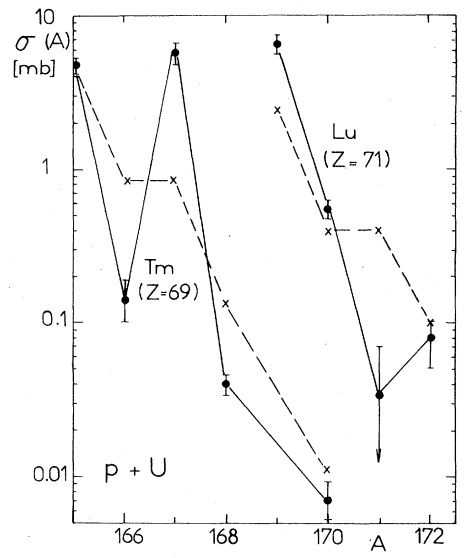

Fig. 8. Spallation of uranium by 28 GeV protons leading to lutetium and thulium isotopes (Ref. 26). The experimental cross sections (solid points) are compared with the predictions, using the two-parameter level density formula Eq. (4.3) and including the memory effect. The absolute value is adjusted, the relative isotope and element distributions are calculated.

V. CONCLUSION

A theory has been formulated using the physical ideas of the two-step model for fragmentation-spallation reactions. Analytical formulas are derived for the mass yield curve $\sigma(A)$ and for the isobaric and isotopic distributions $\sigma(A,I)$. The mass yield curve reflects directly the distribution of excitation energies in the prefragments (i.e., after the first fast stage of the reaction). The isobaric and isotopic distributions are largely determined by the level density of the final product at the particle threshold and are rather insensitive to the initial conditions. The bell shaped distribution functions reflect the shape of the valley of stability. The distributions. retain some memory as to the prefragment distribution. This memory is weak and cannot be used to learn about details of the prefragment distribution (or to determine whether there has been intermediary fission). The fission channel as well as recoil properties of the fragments are outside the treatment. Overall the comparison between experiment and theory is satisfactory. But there are systematic discrepancies: Usually, even-odd effects are more pronounced in the prediction. This may be due to the inadequate formulas for the level density rather than to a failure of the theory itself. At the neutron-rich and the neutron-poor of the isobaric and isotopic distributions, the discrepancies increase. Most probably because of the low particle thresholds the relevant level densities become so small that properties of individual levels dominate and a statistical description breaks down.

ACKNOWLEDGMENTS

Special thanks go to M. Epherre who introduced us to the field of fragmentation-spallation reactions and made us curious. She also helped at various stages of the work. H. Horner showed us the derivation of Eq. (3.6) form the time-dependent master equation. We thank him, A. Abul-Magd, and H. J. Pirner for several discussions. This work was supported in part by the German Federal Ministry of Research and Technology (BMFT) and in part by the Alexander von Humboldt Foundation.

APPENDIX: The solution of the master equation

We start from the master equation in the form (3.6) of an integral equation

$$W(\vec{x})\int d\vec{y}\; M(\vec{x}\to\vec{y})\frac{\Omega(\vec{y})}{\Omega(\vec{x})} - \int d\vec{y}\; W(\vec{y})M(\vec{y}\to\vec{x}) = \frac{P(\vec{x};0)}{\Omega(\vec{x})}\ . \tag{A1}$$

If $M(\vec{x}\to\vec{y})$ depends only on the difference $\vec{x}-\vec{y}$ and if the derivatives of the entropy, Eq. (3.8), do not vary with $\vec{x}$, then

$$\rho = \int d\vec{y}\; M(\vec{x}\to\vec{y})\frac{\Omega(\vec{y})}{\Omega(\vec{x})} \tag{A2}$$

is constant with the value

$$\rho \approx \exp(\beta\epsilon - \mu\alpha);\ \ \mu = (\mu_N + \mu_Z)/2\ . \tag{A3}$$

The constants ϵ and α are defined in Eqs. (3.10) and (3.12), respectively. We normalized $\int d\vec{z}\; M(\vec{z}) = 1$,

thus redefining the time scale. After having isolated a scale factor

$$W(\vec{y}) = c^{y_0} W(\vec{y}) \tag{A4}$$

the function $W(\vec{y})$ is smooth and may be approximated by its Taylor expansion. Then

$$\rho c^{x_0} W(\vec{x}) - c^{x_0+\alpha} \int dy [W(\vec{x}) + (\vec{y}-\vec{x}) \frac{\partial}{\partial \vec{x}} W(\vec{x}) + \ldots] M(\vec{y} \to \vec{x}) = \frac{P(\vec{x};0)}{\Omega(\vec{x})} . \tag{A5}$$

The constant c is chosen to cancel the two terms in $W(\vec{x})$ on the rhs of Eq. (A5). If only the first derivatives in $W(\vec{x})$ are kept, the function

$$W(A,E) = \sum_I W(A,I,E) \tag{A6}$$

satisfies the differential equation

$$\alpha \frac{\partial}{\partial A} W(A,E) + \epsilon \frac{\partial}{\partial E} W(A,E) = \delta_{A,A_0} \frac{P(A_0,I_0,E;0)}{\Omega(A_0,I_0,E)} \rho^{1+A_0/\alpha} . \tag{A7}$$

Because of $\tau_1 = 0$ [Eq. (3.11)] there is no linear derivative in I. The solution of (A7) is given by

$$W(A,E) = \Theta(A_0 - A) \frac{1}{\alpha} \frac{P(A_0,I_0,E + \epsilon(A_0 - A)/\alpha;0)}{\Omega(A_0,I_0,E + \epsilon(A_0 - A)/\alpha) \rho^{1+A_0/\alpha}} . \tag{A8}$$

If we use the approximation

$$\Omega(A,E) = \exp[\beta(E - \mu A)] \tag{A9}$$

with constant values β^{-1} and μ, all level density factors cancel and one arrives at Eq. (3.14).

In order to include some features in the evolution of the neutron excess I, we go to second derivatives, but retain only the term $\frac{1}{2}\tau_2 \partial^2/\partial I^2 \, W(A,I,E)$. The neglect of all other second derivatives like $\partial^2/\partial E^2 \, W$ or $(\partial^2/\partial E \partial I) W$ is only justified *a posteriori* by the relative success of our solution when comparing it with experiment. The equation

$$\left[\alpha \frac{\partial}{\partial A} + \epsilon \frac{\partial}{\partial E} + \frac{\tau_2}{2} \frac{\partial^2}{\partial I^2} \right] W(A,I,E) = \delta_{A,A_0} \delta_{I,I_0} \frac{P(A,I_0,E;0)}{\Omega(A_0,I_0,E)} \rho^{1+A_0/\alpha} \tag{A10}$$

is solved exactly by Fourier or Laplace transform. The physics of the additional term can be made transparent by throwing away all inessentials in Eq. (A10):

$$\alpha \frac{\partial}{\partial A} W(A,I) + \frac{\tau_2}{2} \frac{\partial^2}{\partial I^2} W(A,I) = \delta_{A,A_0} \delta_{I,I_0} . \tag{A11}$$

This is a diffusion equation in the neutron excess I, where A/α plays the role of a negative time. The solution of this equation is the Gaussian appearing in Eq. (3.16).

---

*Permanent address: Division de Physique Théorique, Institute de Physique Nucléaire, F-91406 Orsay, France.

[1]S. B. Kaufman, E. P. Steinberg, B. D. Wilkins, and D. J. Henderson, Phys. Rev. C 22, 1897 (1980).

[2]D. J. Morrissey, W. Loveland, M. de Saint Simon, and G. T. Seaborg, Phys. Rev. C 21, 1783 (1980).

[3]M. Lagarde-Simonoff and G. N. Simonoff, Phys. Rev. C 20, 1498 (1979).

[4]S. Regnier, Phys. Rev. C 20, 1517 (1979).

[5]N. T. Porile, G. D. Cole, and C. R. Rudy, Phys. Rev. C 19, 2288 (1979).

[6]*Spallation Nuclear Reactions and Their Applications,* edited by B. S. P. Shen and M. Merker, Astrophysics and Space Science Library (Reidel, Dortrecht, (1976) Vol. 59.

[7]B. D. Wilkins, S. B. Kaufman, E. P. Steinberg, J. A. Urbon, and D. J. Henderson, Phys. Rev. Lett. 43,

1080 (1979).
[8]N. T. Porile and L. B. Church, Phys. Rev. 133, B310 (1964).
[9]T. H. Ku and P. J. Karol, Phys. Rev. C 16, 1984 (1977).
[10]G. Rudstam, Z. Naturforsch. 219, 1027 (1966).
[11]R. Silberberg and C. H. Tsao, Astrophys. J. Suppl. Ser. 220, 25, 315 (1973); 25, 335 (1973).
[12]V. I. Bogatin, O. V. Lozhkin, and Y. P. Yakovlev, Nucl. Phys. A326, 508 (1979).
[13]V. V. Avdeichikov, Phys. Lett. 92B, 74 (1980).
[14]R. Serber, Phys. Rev. 72, 1114 (1947).
[15]H. W. Bertini, A. H. Culkowski, O. W. Hermann, N. B. Gove, and M. P. Guthrie, Phys. Rev. C 17, 1382 (1978).
[16]I. Dostrovsky, Z. Fraenkel, and G. Friedlander, Phys. Rev. 116, 683 (1959).
[17]R. J. Glauber and G. Matthiae, Nucl. Phys. B 21, 135 (1970).
[18]J. Hüfner, K. Schäfer, and B. Schürmann, Phys. Rev. C 12, 1888 (1975).
[19]K. J. Le Couteur, in *Nuclear Reactions,* edited by P. M. Endt and M. Demeur (North-Holland, Amsterdam, 1959), p. 318.
[20]P. M. Endt and C. van der Leun, Nucl. Phys. A310, 1 (1978).
[21]A. Bohr and B. Mottelson, *Nuclear Structure* (Benjamin, New York, 1969), Vol. I, p. 281.
[22]C. Thibault, M. Epherre, G. Audi, R. Klapisch, G. Huber, F. Touchard, D. Guillemaud, and F. Naulin, in *Atomic Masses and Fundamental Constants 6,* edited by J. A. Nolen and W. Beneson (Plenum, New York, 1980), p. 291.
[23]R. Klapisch, C. Thibault, A. M. Poskanzer, R. Prieels, C. Rigaud, and E. Roeckl, Phys. Rev. Lett. 29, 1254 (1972).
[24]A. H. Wapstra and K. Bos, At. Data Nucl. Data Tables 19, 177 (1977).
[25]Y. P. Viyogi, T. J. M. Symons, P. Doll, D. E. Greiner, H. H. Heckman, D. L. Hendrie, P. J. Lindstrom, J. Mahoney, D. K. Scott, K. van Bibber, G. D. Westfall, H. Wieman, H. J. Crawford, C. McParland, and C. K. Gelbke, Phys. Rev. Lett. 42, 33 (1979).
[26]Y. Y. Chu, E. M. Franz. G. Friedlander, and P. J. Karol, Phys. Rev. C 4, 2202 (1971).